Colloid & Polymer Science Colloid Polym Sci 269:375–391 (1991)

Conformational motion and disorder in aliphatic nylons The case of nylon 6.6*)

A. Xenopoulos and B. Wunderlich

Department of Chemistry, University of Tennessee, Knoxville, Tennessee, and Chemistry Division, Oak Ridge National Laboratory, Oak Ridge, Tennessee, USA

Abstract: On the basis of thermal analysis it is suggested that the crystals of aliphatic nylons exhibit conformational disorder above the glass transition. The disorder begins gradually at about room temperature and is evidenced by an increase of the heat capacity to values higher than that of the melt. The specific case of nylon 6.6 is investigated by thermal analysis and x-ray diffraction. The onset of conformational disorder can be clearly separated from premelting. It is shown that the Brill transition, as defined by the merging of the two main peaks in the x-ray diffraction pattern, occurs gradually and is thermal-history-dependent. The transition is not a first-order one, it is only an incidental thermal effect, associated with a packing change in the crystal. In solution-crystallized (sc) samples this change is related to a distinct endothermic peak, while in melt-crystallized (mc) samples it is related to a broad endotherm.

Key words: Nylon, heat capacity; conformational disorder; Brill transition.

Introduction

Aliphatic nylons have received considerable interest over the years in terms of both their structure [1] and their transition behavior [2]. A complicated picture has emerged, including polymorphism [3], multiple melting [4], reorganization on heating [5], lamellar thickening [6] and increased mobility at higher temperatures [7]. We have undertaken detailed investigations on the thermodynamic properties of the aliphatic nylons. A fundamental understanding of the behavior of semicrystalline samples requires the knowledge of the two limiting states of the polymer, the fully crystalline and the fully amorphous one. The heat capacities (C_p) of seven solid nylons (nylon 6, nylon 11, nylon 12, nylon 6.6, nylon 6.9, nylon 6.10 and nylon 6.12) were recently calculated based on approximate vibrational spectra fitted at one or two temperatures to the experimental heat capacities [8]. The C_p of the melts was measured, and an addition scheme was developed to predict them for any other nylon [9]. Based on this knowledge a comparison was possible between the experimental C_p of semicrystalline polymers and the C_p predicted, assuming additive contributions of the crystalline and the amorphous portions (two-phase crystallinity model) [9]. For all the cases analyzed the experimental C_p reaches the values of the liquid 70 to 150 K below the melting temperature. This high value is shown to be related to the onset of conformational motion and disorder. This effect could be separated from premelting, recrystallization, and reorganization of poor crystals. The possibility of condis nylons was first suggested [10] based on reports of the possible existence of extended-chain crystals of nylons.

In the case of nylon 6.6 a transition occurs below melting, the Brill transition. The initial observation of this transition was made in 1942, when Brill re-

*) Dedicated to Professor Dr. W. Pechhold on the occasion of his 60th birthday

ported [11] the merging of the two strongest x-ray diffraction peaks of nylon 6.6, the 100 and 010 reflections, into one single peak at 435 K. Nylon 6 did not show a similar merging. The transformation occurred already at 415 K in the presence of water vapor. It was shown to involve a change from a triclinic crystal structure to a pseudohexagonal one. It was later suggested that the essentially two-dimensional hydrogen-bonded sheets transform, above the transition, into a dynamical three-dimensional hydrogen bond network [12]. The dynamic nature of the transition was then studied by proton NMR [7]. The abrupt narrowing of the line-width in the NMR spectrum was interpreted as the onset of torsional and rotational motion in the paraffinic segments of the nylons. The temperature where the narrowing occurs corresponds to the temperature of the crystallographic change. The transition occurs at lower temperatures for odd-odd compared to even-even nylons, and it is found also at lower temperatures for longer methylene sequences due to the smaller constraints on the methylenes. Additional wide-line NMR experiments were performed on drawn nylon 6.6 monofilaments [13]. The observed decrease in second moment at 450 K was explained by a "60° flip-flop" mechanism (rotational jumps of 60° about the long axis with breaking and reforming of the hydrogen bonds) with superimposed large-amplitude oscillations of the CH_2 groups. The latter point was recently investigated by deuterium NMR and molecular dynamics simulations [14]. Both methods demonstrate that individual methylene groups within the crystals exhibit large-amplitude librational motion well below the melting point.

The Brill transition endotherm was evident in DSC traces of samples crystallized from methanol as opposed to melt-crystallized samples [15]. A latent heat of 4.26 kJ/mol was reported for the transition. Deconvolution of the excess heat capacity of the Brill transition in nylon 6.6, based on a two-state statistical mechanics model [16] suggested that the transition involves about 25 repeat units or about five stems in a folded-chain crystal, a segment much smaller than the size of the crystal.

In the present work, we compare the thermal properties of solution-crystallized and melt-crystallized samples of nylon 6.6 (hereafter denoted as sc and mc, respectively). We also describe the effect of thermal history on thermal properties and crystal structure. The purpose is to elucidate the relation between motion in the crystal and the Brill transition.

Experimental

Materials

For some of the nylon 6.6 experiments (runs *m*1, *m*2 and *m*3 in Table 1), we used samples purchased from Scientific Polymer Products, Inc.. All were free of additives and have very low monomer content, as stated by the meanufacturer. Molecular weights were not determined, but are typically in the range 15 000–25 000. For the solution crystallization, the remaining DSC experiments and the WAXD experiments on nylon 6.6, commercial Zytel pellets were used purchased from DuPont. Before the DSC experiments all samples were dried overnight in a vacuum oven; they are kept at all times in a sealed desiccator.

*The index *i* refers to either rate or temperature and corresponds to the index in the "Experiment".

Table 1. Description of nylon 6.6 DSC experiments*

Experiment	Experimental details before analysis at 10 K/min
*m*1-*i*	Heated to 560 K, kept for 5–10 min and cooled to 220 K at rate *i* K/min or quenched in liquid nitrogen (*i*=Q)
*m*2-*i*	Heated to 560 K, cooled to T_i at 320 K/min, kept for 30 min and cooled to 210 K at 320 K/min
*m*3-*i*	Heated to 560 K, kept for 5–10 min, cooled to 250 K at 20 K/min, kept for 1–2 min, cooled to 250 K at 20 K/min and reheated to a T_i lower by 10 K
*m*4-*i*	Enclosed in a glass tube under vacuum, heated to 570 K in a sandbed and: annealed overnight at 493 K and cooled slowly (*i*=1); cooled abruptly to room temperature (*i*=2); quenched to liquid nitrogen (*i*=3)
*m*7	Dried in an air oven at 390 K for 2 hours, brought to room temperature and cooled to 243 K at 5 K/min
*m*8	Heated to 493 K at 10 K/min, kept for 17 hours and cooled to 243 K at 0.5 K/min
*m*9	Held in a desiccator over P_2O_5
*m*10-*i*	heated to 573 K at 20 K/min, kept for 5–10 min and cooled to 233 K at rate *i* K/min
*s*1-*i*	Heated to T_i at 10 K/min, kept for 30 min and cooled to 263 K at 500 K/min
*s*2-*i*	Heated to T_i at 500 K/min, kept for 30 min and cooled to 263 K at 500 K/min
*s*3 and *m*5	Kept in a desiccator over drierite and cooled from room temperature to 253 K at 5 K/min
*s*4 and *m*6	Kept in a desiccator over P_2O_5 and cooled from room temperature to 243 K at 5 K/min
*s*5	Heated to 493 K at 10 K/min, kept for a total of 26 hours and cooled to 243 K at 0.5 K/min
*s*6	Heated to 493 K at 10 K/min, kept for 2 min, cooled to 243 K at 10 K/min and repeated
*s*7-*i*	Heated to 493 K at 10 K/min, kept for 30 min and cooled to 243 K at rate *i* K/min

For the solution crystallization, following Starkweather [15], nylon 6.6 pellets were dissolved in ethylene glycol. The concentration was approximately 50 g/l and the dissolution temperature about 450 K. On cooling a thick gel precipitated around 420 K; this was vacuum-filtered and washed with excess of doubly distilled water to remove the high-boiling point ethylene glycol. The thick, wet powder obtained was then ground and dehydrated over P_2O_5 in a vacuum desiccator and finally dried in a vacuum oven at 380 K to produce a fine powder.

A fine powder was also obtained from the nylon 6.6 (Zytel) pellets using a commercial Tekmar analytical grinding mill, which was used in experiments *m*4 to *m*10 in Table 1. A few grams of the pellets were cooled with liquid nitrogen and immediately transferred into the mill chamber where a blade turned at 20 000 rpm. The resulting product was passed through a sieve to give a fine powder; it was also dried in a vacuum oven at 380 K and subsequently kept inside a desiccator.

The crystallinities of the samples were determined from their measured heats of fusion, using 57.4 kJ/mol for the completely crystalline nylon 6.6 [17].

Equipment

All DSC experiments described in this paper were performed on two Perkin-Elmer instruments, DSC-2 and DSC-7. The DSC-2 and its operation have been described in detail earlier [18]. The DSC-7 was interfaced with a Perkin-Elmer Model 7500 computer. The software used is proprietary to Perkin-Elmer and very little information exists about the specific algorithms used for the calculation of the heat capacity. No standard is used for the calculation. Our own measurements of standard sapphire (Al_2O_3) showed the C_p obtained to be on the average 5 % lower than the literature data [19]. It was thus deemed necessary for all measurements to use an additional run with sapphire and to correct the results obtained by the Perkin-Elmer software using the literature sapphire C_p data. Calibration of the temperature and heat of fusion is done automatically using two and one standards, respectively. We used indium and naphthalene for temperature, and indium for heat of fusion. The thermal lag is also internally corrected using the leading slope of the indium melting curve. For low-temperature operation mechanical refrigeration is used (Perkin-Elmer intracooler). The DSC cell is thermostatted at 190 K which allows for operation of the DSC at about 220 K. Two h of equilibration are needed for the heat flow signal to reach a constant value before starting the experiment. The mechanical refrigeration provides a stable block temperature and is also used for ambient operation in order to get stable, reproducible isotherms.

The Perkin-Elmer dry box is used in order to avoid signal instability due to drafts or room temperature changes. In addition, a constant, low pressure of dry nitrogen gas is kept in the dry box in order to avoid water condensation. The design of the dry box was found, however, to allow large nitrogen leaks and special covers were designed and placed on the dry box to ensure sealing. A drying agent was kept permanently inside the dry box to absorb whatever moisture was still present. Dry nitrogen gas was also flowing through the DSC cell at a flow rate of 20 ml/min. The heat capacity runs were performed on 15–25 mg samples. It was ensured that the aluminum pans used for all three runs (sample, blank, and reference) were of the same weight within ± 0.05 mg. The typical heating rate is 10 K/min.

The Wide Angle X-ray powder Diffraction (WAXD) experiments described were performed on two instruments, a Rigaku diffractometer at the University of Akron and a Scintag diffractometer at Oak Ridge National Laboratory. The Rigaku instrument had a 12-kW rotating anode as a source of the incident x-ray beam. The line-focused beam is monochromatized with a graphite crystal and a pulse-height analyzer to CuK_α radiation. A D/Max-B x-ray powder diffractometer was controlled by an IBM personal computer. The temperature controller used had a precision of ± 0.1 K in the temperature range between room temperature and 620 K. The Scintag PADV instrument is based on the MZV-105 diffractometer. The source of x-rays is a 3-kW generator with CuK_α radiation. The instrument is controlled by a DMC-105 microcomputer and uses XDS software by the same company. The temperature control unit HTC 3000 could go up to 3000 K and had a precision of ± 1 K in the temperature range measured.

Results

X-ray diffraction data

The Brill transition is recognized crystallographically as the merging of the two main reflections with increasing temperature. An easily identifiable endothermic DSC peak is only associated with the transition in the case of samples crystallized from solution, as was detailed in the Introduction. We investigated the behavior of two different types of mc samples by obtaining x-ray patterns at various temperatures, in order to be able to relate the crystallographic data to the thermal analysis results.

The first set of experiments was performed on ground powder of 29 % crystallinity using the ORNL instrument, as described in the Experimental part. The heating and cooling curves from this experiment are shown in Fig. 1. The sample was heated to 493 K, about 40 K below the melting peak. The high-temperature form has a (100)-spacing of 0.42 nm. Only an approximate transition temperature can be obtained from the data collected on heating (Fig. 1a) as the peak at 493 K is already very sharp. The pattern at 493 K is somewhat asymmetric. An additional characteristic of the 493 K x-ray pattern is the sharpening of a small peak corresponding to a spacing of 0.66 nm. The x-ray pattern does not change after keeping the sample at 493 K for 1.5 h. On cooling (Fig. 1b) a double peak starts to emerge at about 380 K. The separation of the two peaks is complete at room temperature. The resulting pattern, however, is slightly different from that of the initial sample, as can be seen by the comparison shown in Fig. 2a. The high-2 θ 010, 110 reflection is more prominent than before heating. This change in relative intensities is reversed if, on heating, we reach a higher temperature, namely 523 K, as can be seen in Figure 2b. The

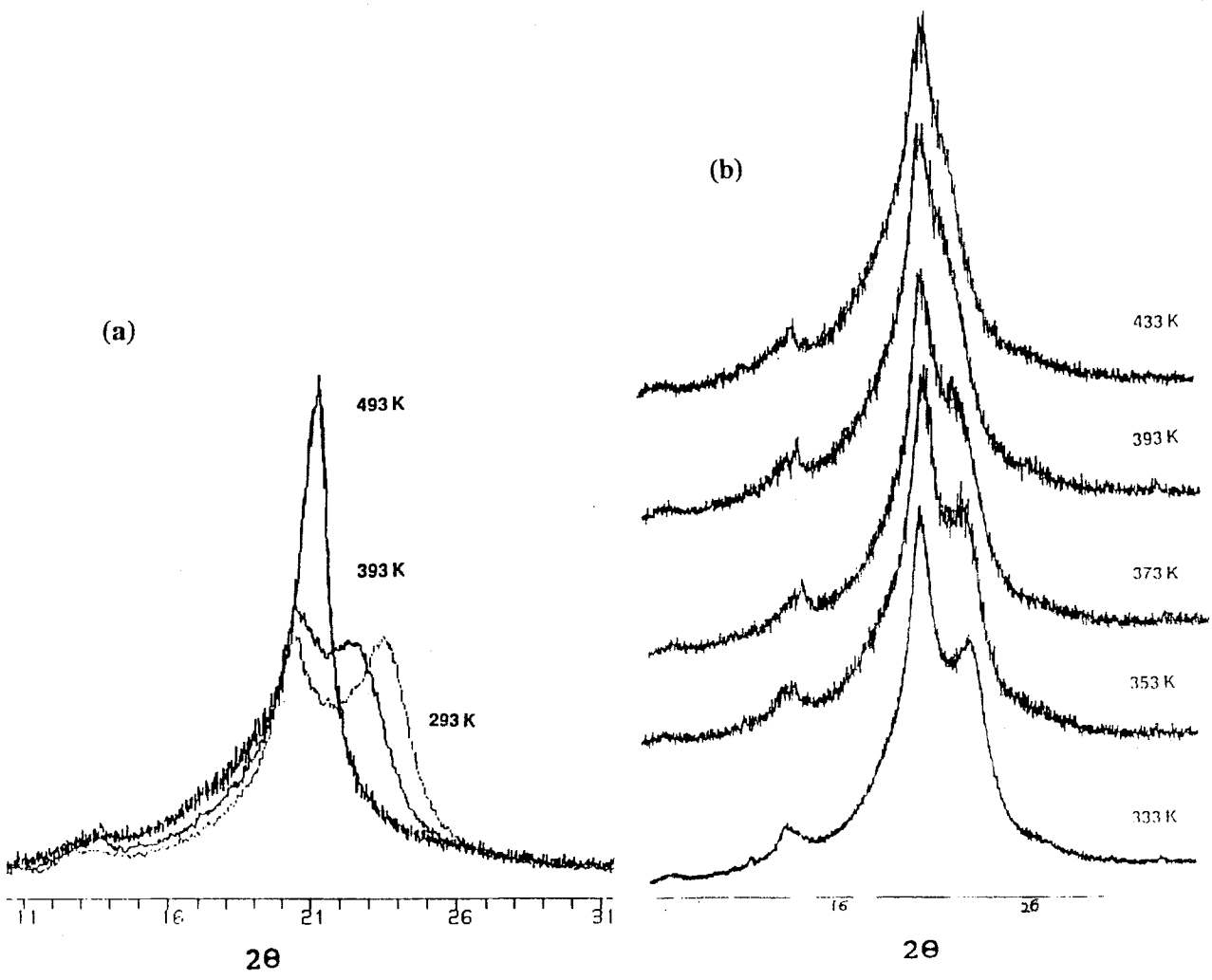

Fig. 1. WAXD experiments on melt-crystallized nylon 6.6 powder; a) heating curves, b) cooling curves

010, 110 reflection is now lower in intensity than in the sample that had not been heated.

The second set of experiments was performed on quenched samples using the Rigaku diffractometer, as was also described in the Experimental part. The patterns obtained on heating are shown in Figure 3a. The merging of the diffraction peaks occurs between 380 K and 400 K and the highest temperature reached in this experiment is 460 K. On subsequent cooling (Fig. 3b) the splitting of the single peak occurs between 430 K and 410 K. The final x-ray diffraction pattern is identical to the initial one. The 010, 110 reflection, corresponding to a *d*-spacing of 0.38 nm has a larger intensity than the 100 reflection, that corresponds to a *d*-spacing of 0.45 nm.

Differential scanning calorimetry data

All samples of nylon 6.6 that were used in this research were described in the Experimental part and fall into two categories: melt-crystallized and solution-crystallized. The experimental details for each particular run are given in Table 1. Experiments identified with a first letter "s" refer to sc samples while a first letter "m" refers to mc samples. The relevant results on transition parameters are listed in Table 2 and 3, for the sc and mc samples, respectively.

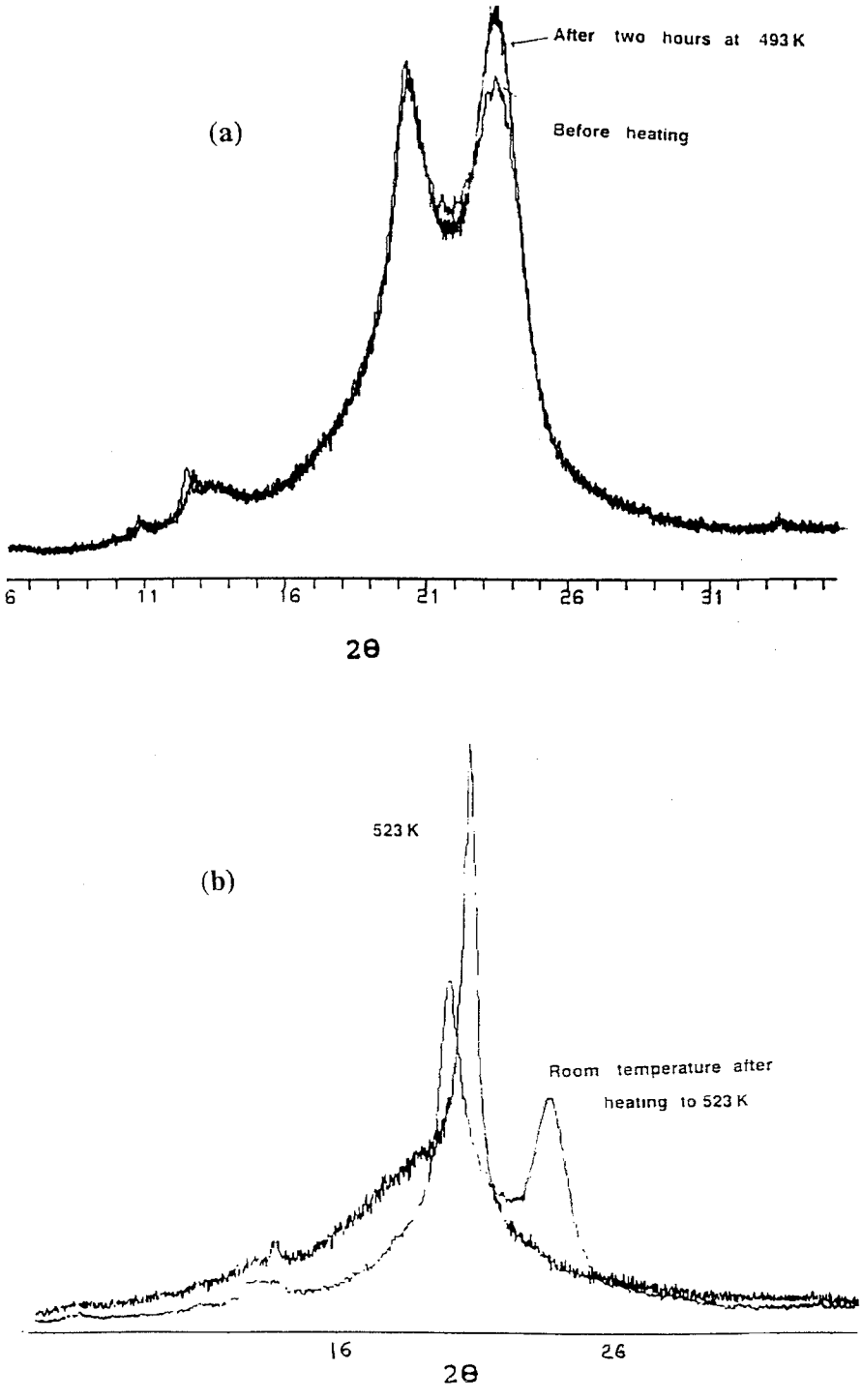

Fig. 2. Effect of the highest temperature reached on room temperature x-ray diffraction patterns of nylon 6.6. a) T_{max} = 493 K (see Fig. 1a for the trace at 493 K); b) T_{max} = 523 K

Table 2. Transition parameters for solution-crystallized nylon 6.6 samples*

Run No.	T_m(K)	T_B(K)	T_m'(K)	ΔT_m(K)	ΔT_B(K)	ΔH_m	ΔH_B	ΔH_t
*s*1-500	539.3	465	532	49	66	25.7	2.9	28.6
*s*1-490	540.5	465	532	53	63	25.2	2.6	27.8
*s*1-480	539.3	464	532	60	60	26.9	1.8	28.7
*s*1-470	540.0	475	529.4	49	72	25.2	2.5	27.7
*s*1-460	539.5	473	533.0	53	59	26.5	2.2	28.7
*s*1-440	539.5	469	531.3	52	66	24.5	2.8	28.3
*s*2-500	539.0	463	529.9	56	69	25.2	2.4	27.6
*s*2-490	538.3	464	528.5	50	60	25.2	2.2	27.4
*s*2-480	538.9	464	529.7	60	60	24.6	1.9	26.5
*s*2-470	538.4	464	529.6	49	64	25.3	2.2	27.5
*s*2-460	540.3	471	531.3	51	65	22.6	2.3	24.9
*s*2-440	538.9	468	528.5	44	62	24.9	2.5	27.4
*s*3	539.5	468	531.1	48	62	25.4	2.6	28.0
*s*4	539.3	469	530.2	52	62	25.0	2.6	27.6
*s*5	531.6	463	–	40	68	26.4	2.5	28.9
*s*6	538.7	464	534	55	74	24.8	2.7	27.5
*s*7-500	538.2	464	533	43	74	25.2	2.5	27.7
*s*7-120	538.4	463	533	51	85	25.6	2.8	28.4
*s*7-40	538.1	464	534	48	78	25.6	2.6	28.2

*A subscript "B" refers to the Brill transition; T_m' refers to other endothermic peaks; ΔH_t is the sum of ΔH_m and ΔH_B; all ΔH values are in kJ/mol.

Although the Brill transition occurs – according to the x-ray data – in both the mc (see previous section) and sc (see [15]) nylon 6.6 samples, a clearly separable endothermic effect is only observed in the DSC traces of the sc samples. From all runs included in Table 2 we can obtain average Brill transition parameters for the solution-grown crystals, namely 466.4 ± 3.7 K for the peak temperature and 66.4 ± 7.0 K for the temperature ranges of the transition and 2.44 ± 0.30 kJ/mol for the latent heat of the transition. The melting peak is a double peak for all runs except *s*5, where the sample was annealed for many hours. Apart from this run on the annealed sample, the average peak melting temperature is 539.1 ± 0.7 K, the average melting range 51.3 ± 4.6 K and the average heat of fusion 25.2 ± 0.9 kJ/mol. From this value we can calculate an average crystallinity for all sc samples of 44 %. Adding ΔH_m and ΔH_{Brill} gives an average ΔH_{total} for all runs of 27.7 ± 0.9 kJ/mol. The low-temperature shoulder of the melting peak ranges from 529.7 K to 534 K.

In experiment *s*1 the samples were heated slowly (10 K/min) to the annealing temperature T_a, while in experiment *s*2 they were heated as fast as possible (about 500 K/min). There are some systematic differences between the two experiments, both average transition temperatures and heats of transition being higher for *s*1. More specifically, for the melting transition the differences are 0.7 K and 1.0 kJ/mol and for the Brill transition, 2.8 K and 0.22 kJ/mol, respectively. An additional difference is that the low-temperature shoulder is more pronounced in the case of *s*2. Within each set of experiments there seems to exist no trend in the melting peak temperatures or heats of transition. The Brill transition, however, in *s*1 has a maximum in temperature for T_a = 470 K and a minimum in heat of transition for T_a = 480 K. In the case of *s*2 there is a maximum in T_{Brill} for T_a = 460 K and a minimum in ΔH_{Brill} for T_a = 480 K. The low-temperature shoulder of the melting peak becomes smaller with decreasing T_a.

The two runs without prior annealing (untreated), *s*3 and *s*4 are essentially identical in appearance and transition parameters. In fact, their transition para-

Table 3. Transition parameters for melt-crystallized nylon 6.6 samples*

Run No.	T_m(K)	other T_{endo} (K)	ΔT_m (K)	ΔH_m (kJ/mol)
*m*1-2.5	535.9	525	119	18.1
*m*1-10	534.4	infl. @ 513	134	17.6
*m*1-320	535.0	–	28	13.9
*m*1-Q	536.7	–	32	12.4
*m*2-500	536.1	sh @ 514, peak @ 525	142	not det
*m*2-490	535.2	infl @ 501, peak @ 521	123	16.5
*m*2-480	534.9	infl @ 489, 512	133	16.3
*m*2-470	534.6	infl @ 479, 510	126	15.6
*m*2-460	534.3	infl @ 468, 510	141	not det
*m*2-450	534.2	infl @ 458, 509	125	15.1
*m*2-440	534.1	infl @ 447, 509	142	15.1
*m*2-430	534.0	infl @ 438, 508	132	15.0
*m*2-420	534.0	infl @ 429, 507	133	15.0
*m*2-410	533.8	infl @ 420, 507	139	15.1
*m*2-400	533.6	infl @ 411, 507	144	not det
*m*4-1	542.1	–	28	23.4
*m*4-2	540.7	–	38	18.6
*m*4-3	537.9	infl @ 500	31	15.2
*m*5	534.9	521	56	18.4
*m*6	535.3	522	54	17.9
*m*7	535.5	sh @ 523	68	19.7
*m*8	535.8	528	58	22.4
*m*9	534.8	sh @ 527	44	16.8
*m*10-500	535.5	infl @ 507	55	13.9
*m*10-200	535.2	infl @ 507	55	14.2
*m*10-80	535.1	infl @ 512	55	14.4
*m*10-40	534.6	sh @ 527	55	14.8
*m*10-20	534.2	sh @ 525	55	14.8
*m*10-10	533.8	sh @ 527	55	15.0
*m*10-0.4	533.4	–	55	15.3

* "infl" means inflection; "sh" means shoulder; "not det" means that ΔH_m was not determined.

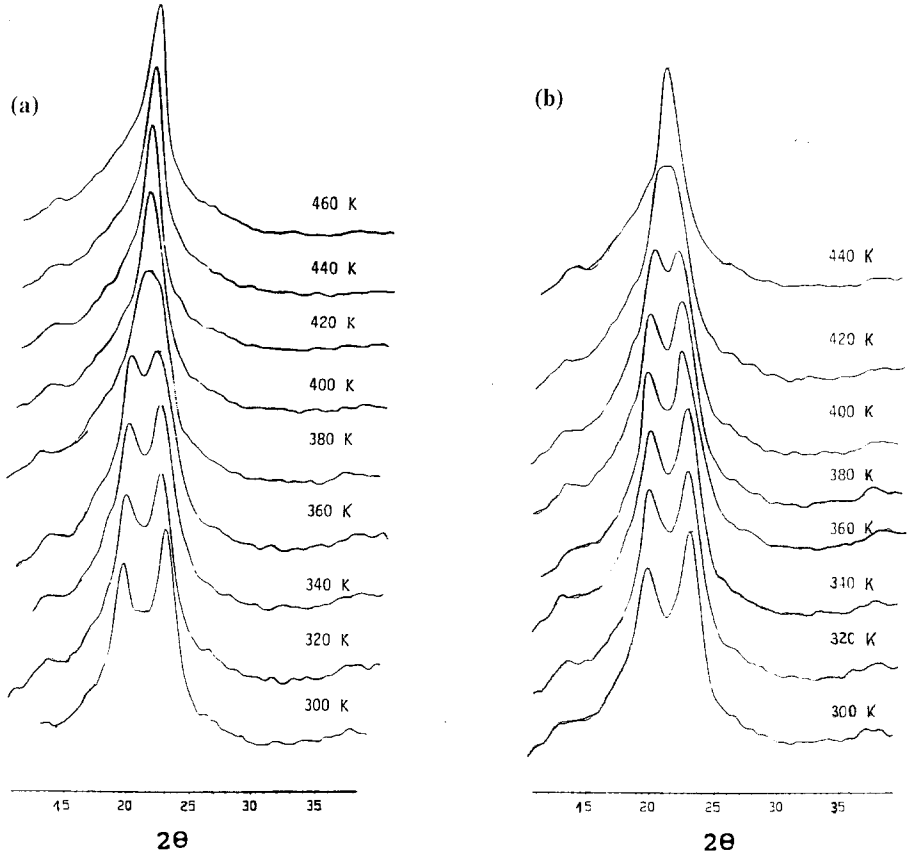

Fig. 3. WAXD experiments on melt-quenched nylon 6.6 a) heating curves,b) cooling curves

meters agree very well with the average values calculated from the data in Table 2.

Long-time annealing has a significant effect on the sample, as can be seen in run *s*5. On initial heating to 493 K, the Brill transition is clearly observed with the expected peak temperature and heat of transition. On subsequent slow cooling there is a very broad exotherm, extending to the lowest temperature, but no secure estimate can be made of the heat associated with it. The DSC trace for the final heating run (Fig. 4) shows that the initial double melting peak has been transformed into a symmetrical single peak with a peak temperature lower by 6.5 K than the lowest peak temperature observed. The melting range is also the narrowest of all runs, while the total heat of transitions is the highest of all. It has to be noted that if ΔH_m without the Brill transition heat is considered, run *s*5 has only the second highest heat of transition. The Brill transition is not at all affected by annealing at a temperature higher than its peak temperature. All its parameters for this series of runs are within the experimental error of the average values.

The repeatability of the Brill transition was checked in run *s*6 by heating to 493 K, cooling after only 2 min at that temperature and then repeating.

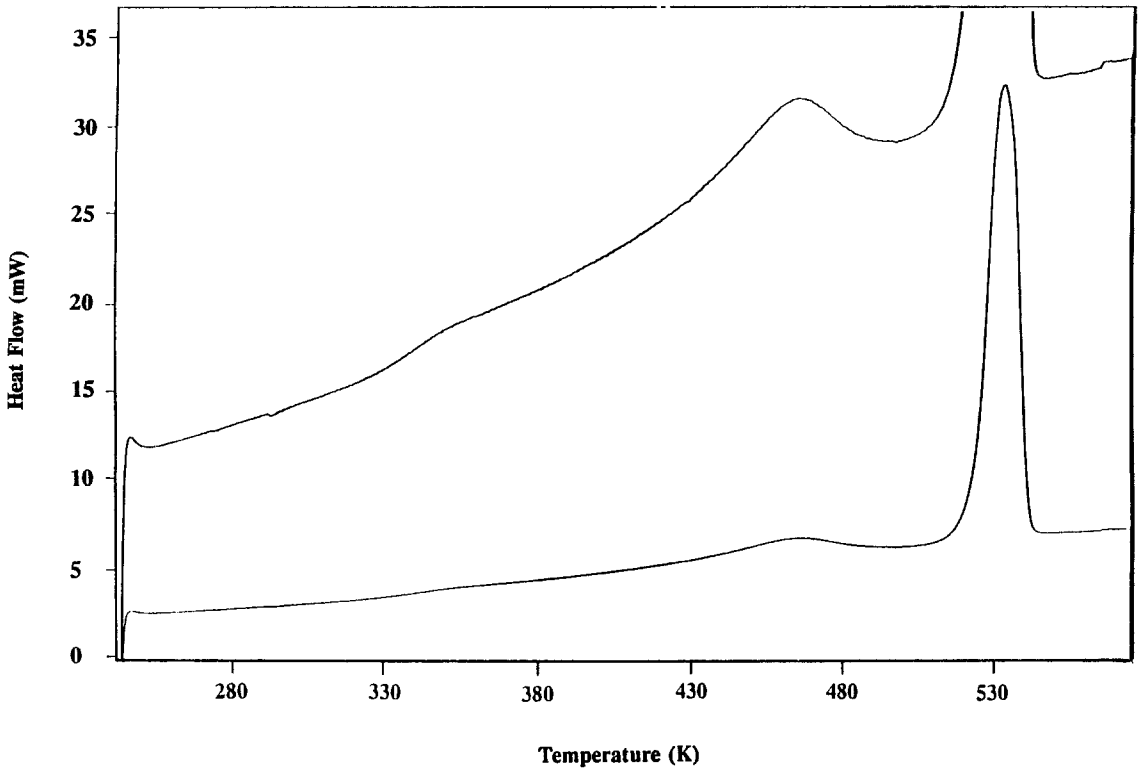

Fig. 4. Experiment *s6*. The trace is shown in two scales and the ordinate refers to the bottom scale

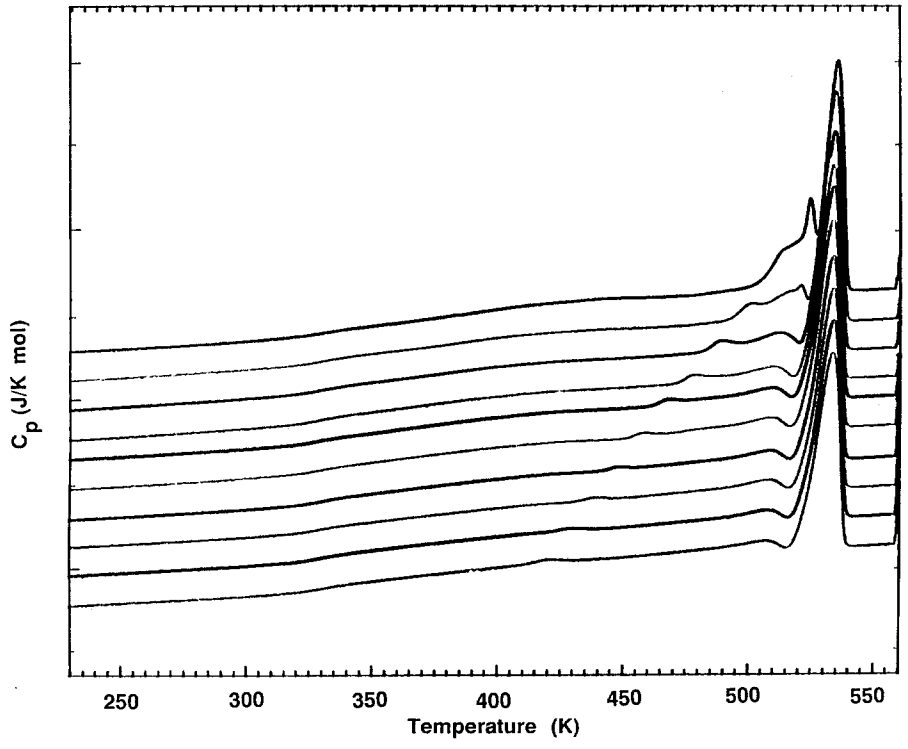

Fig. 5. Experiment *m2*

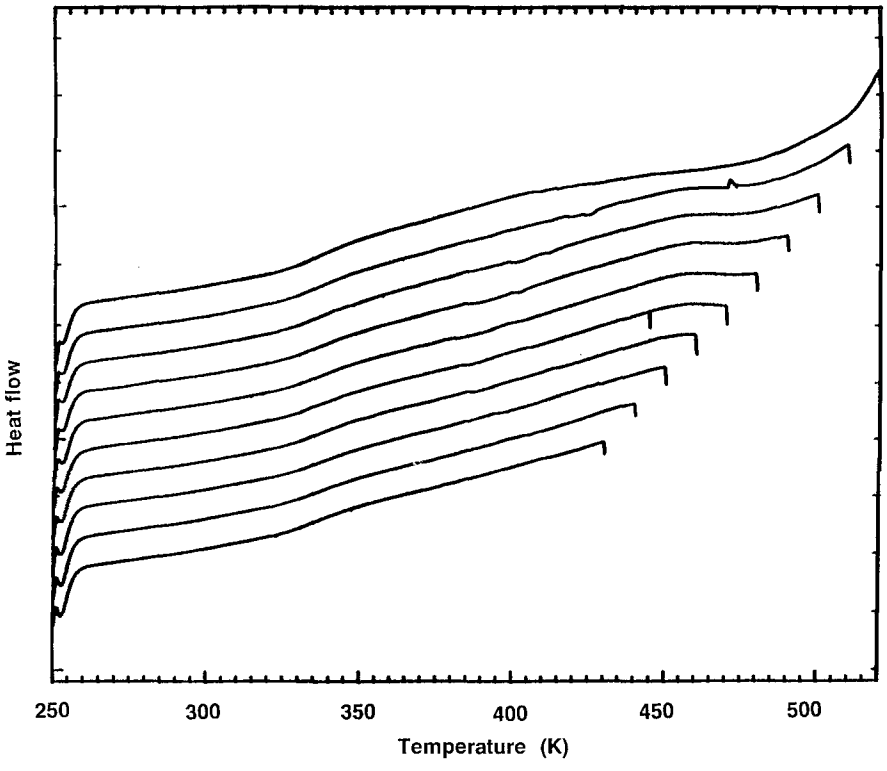

Fig. 6. Experiment *m*3 (heating curves)

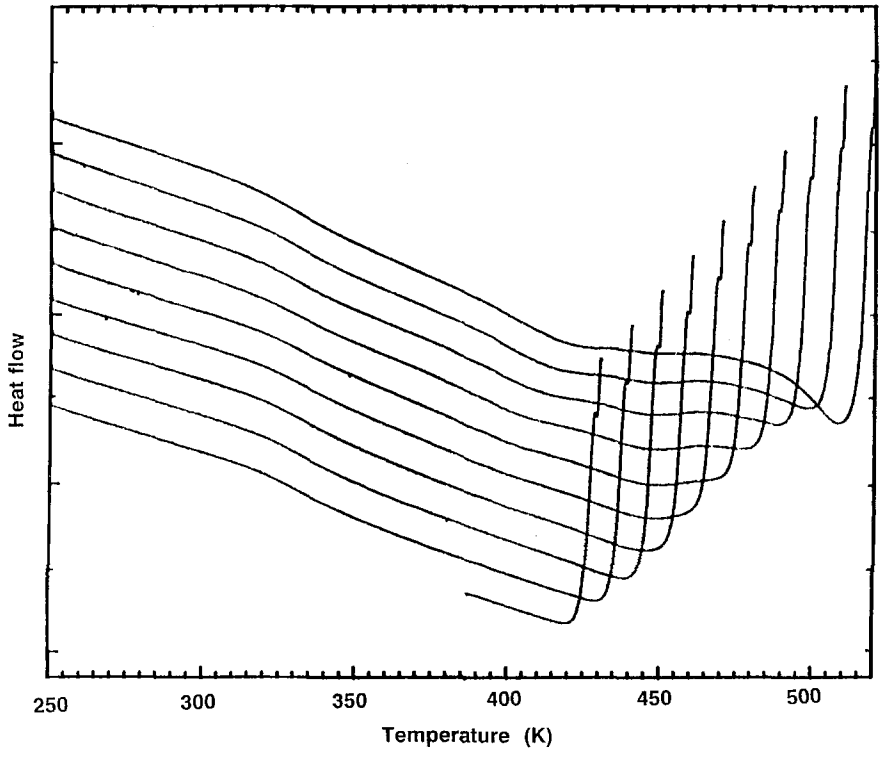

Fig. 7. Experiment *m*3 (cooling curves)

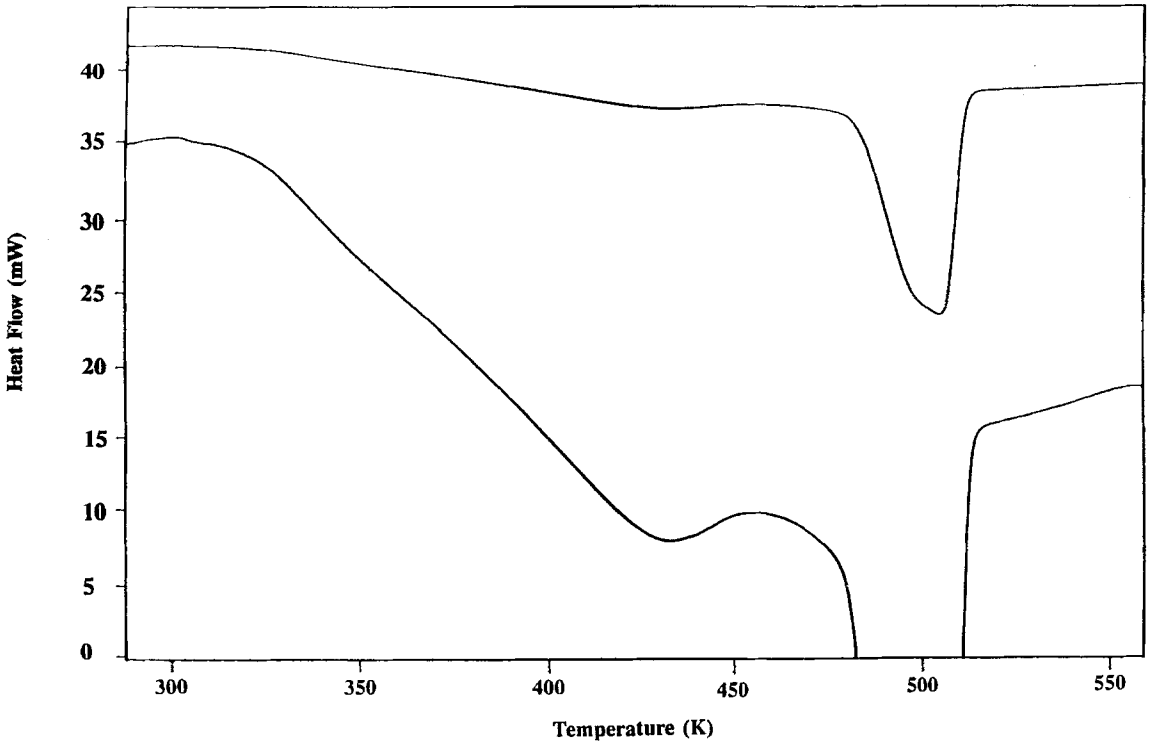

Fig. 8. Experiment *m*10 (cooling curve). The trace is shown in two scales and the ordinate refers to the top scale

The three heating curves are practically indistinguishable except for a more pronounced glass transition for the first heating curve (in fact, a slight endotherm is observed above T_g, which disappears in the last two heating curves). The two cooling curves are also indistinguishable; closer inspection of them indicates a two-step broad endotherm ranging from 484 K to 323 K with a heat of 5.5 kJ/mol. This compares to only 2 kJ/mol, at most, on heating. As the instrument is not calibrated on cooling, the transition heat obtained for broad transitions on cooling is not to be compared quantitatively with heats measured on heating.

The last set of experiments, *s*7, involved different cooling rates after 30 min at 493 K. The three DSC traces obtained are very similar among themselves and with the previous runs. The data in Table 2 do not show any trends of the transition parameters with cooling rate from 493 K.

The mc samples do not have a distinct endotherm in the region of Brill transition, but they are much more affected by different thermal histories. It should be recalled here that, as was described in the Experimental part, experiments *m*1–*m*3 and *m*4–*m*10 were performed on two different kinds of nylon 6.6 samples, respectively. The average melting peak temperature for all runs included in Table 3 is 535.3 ± 1.9 K. The only experiment that deviated significantly from this average was *m*4. The average heat of fusion of all runs was 16.3 ± 2.5 kJ/mol, making the average crystallinity of the samples 28 %.

The first experiment, *m*1, has been already discussed in terms of the melting behavior [9]. The main observations were the gradual disappearance of the low-temperature shoulder of the main melting peak and the decrease of ΔH_m with increasing cooling rate from the melt. In addition, a broad endotherm between T_g and T_m was seen for all four runs, an effect more pronounced in the case of nylon 6.6 when compared to the other nylons discussed [9].

Experiment *m*2 is based on crystallization from the melt at different crystallization temperatures for the same time, 30 min. A composite plot of runs *m*2–500 (top trace) to *m*2–410 (bottom trace) is shown in Fig. 5. It becomes apparent that while the main melting peak stays essentially constant, the region below T_m

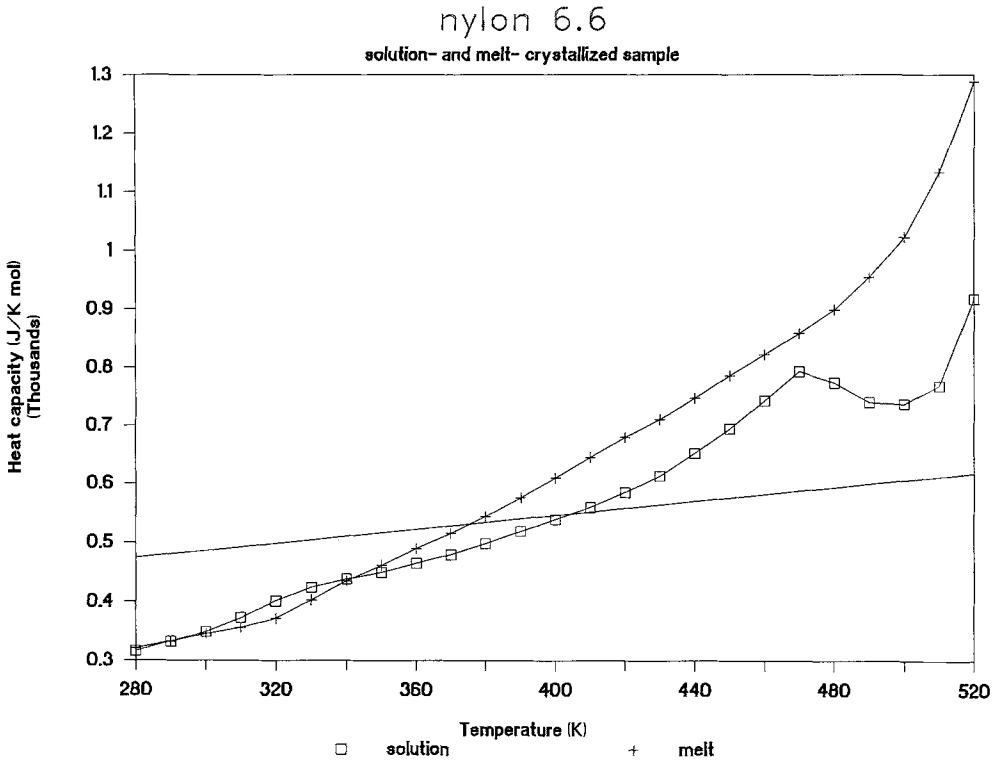

Fig. 9. Comparison of heat capacities of sc and mc nylon 6.6 samples

is drastically affected. The variation of the peak temperatures with the crystallization temperature shows that the low-temperature, small endotherm occurs at a temperature that is always about 10 K higher than the crystallization temperature. The melting range, defined by the intersection of the linear extrapolation of the melt heat capacity with the semicrystalline heat capacity is very wide and practically constant at 135 ± 8 K. The heat of fusion, however, decreases with decreasing crystallization temperature. A closer inspection of the heat capacities in the region between T_g and T_m makes evident the broad endothermic inflection mentioned for experiment *m*1. The inflection is more pronounced for the higher crystallization temperatures.

In experiment *m*3 the sample, after initially erasing its thermal history by melting, was cooled below T_g and then heated to 520 K (just below melting) and immediately cooled down again and reheated to 510 K. This cycling was continued to successively lower temperatures, reaching 430 K. The heat-flow traces on heating are shown in Fig. 6, where the top curve is *m*3–520 and the bottom curve is *m*3–430. The heat-flow traces on cooling are shown in Fig. 7, with *m*3–520 being again the top curve and *m*3–440 the bottom one. The salient feature of these runs is a broad, but distinct endotherm in the region between 410–470 K for runs *m*3–510 through *m*3–470 on heating. The endotherm, if at all present in heating run *m*3–520, is clearly broadened and moved to lower temperatures. A corresponding exotherm is seen at a supercooling of about 30 K for runs *m*3–520 through *m*3–480 on cooling. The areas under the inflections, although not measured, are comparable for the corresponding heating and cooling runs and decrease with decreasing maximum temperature.

Experiments *m*4 are done in a glass tube with gram quantities. In all three runs a single melting peak was obtained, and for the sample quenched in liquid nitrogen a pre-T_m small exotherm appears, but no post-T_g sharp exotherm, as in run *m*1-Q. A very broad endotherm is, in fact, evident in the region between T_g and T_m, reminiscent of experiments *m*1, *m*2, and *m*3. The most significant effect is seen in run *m*4–1, where overnight annealing and subsequent slow cooling increase both T_m and ΔH_m to the highest values in Table 3, 5. 7, 6.6 K and 7 kJ/mol higher than the average values, respectively.

Similar long-time annealing, this time in the DSC cell, was performed in the case of run *m*8. The results were quite different and the measured heat capacity below T_m is shown in Fig. 10. A double melting peak

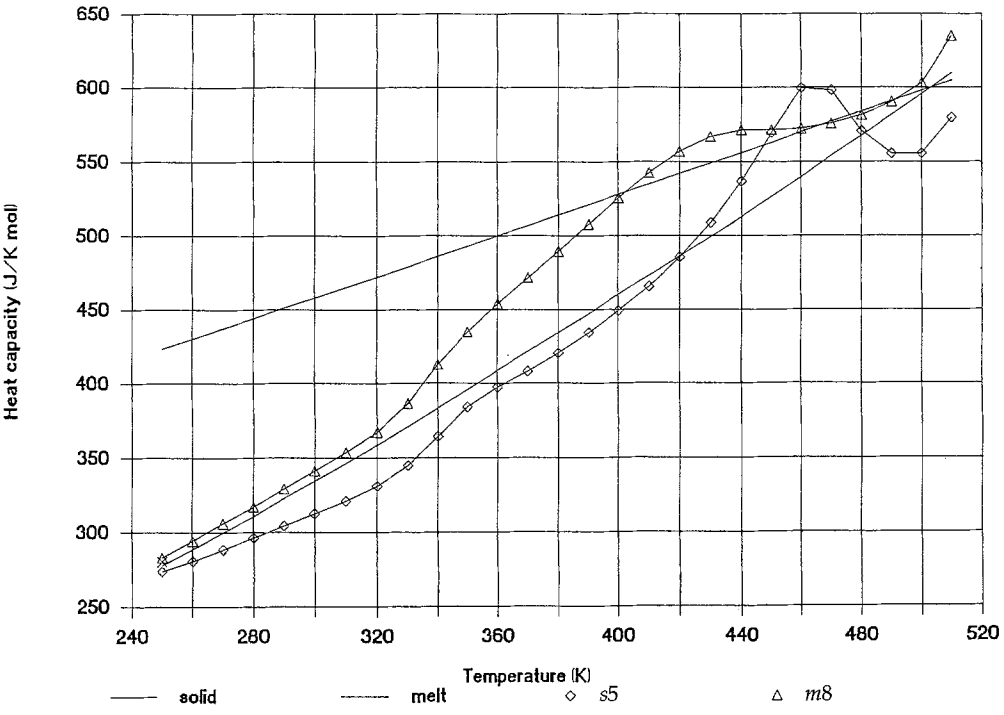

Fig. 10. Heat capacities from experiments *s*5 and *m*8

was obtained, with the low-temperature peak being much more pronounced than in the case of an unannealed sample. The highest peak temperature was not higher than the average value from Table 3, but ΔH_m was almost as high as in the case of *m*4-1. In addition, a broad endotherm developed above T_g. It extends from 360 K to 470 K with a peak temperature of 422 K and a latent heat of 2.2 kJ/mol. The value of the latent heat is almost twice the value of the inflection observed in an unannealed sample.

The last experiment, *m*10, was performed mainly in order to study the cooling curves, but the measured transition parameters for the heating curves are also included in Table 3 for completeness. An example of a sample cooled from the melt at 20 K/min is shown in Fig. 8. The run is shown in two scales in order to emphasize the two-stage crystallization process. An additional experiment was also performed, where a sample was cooled from the melt at 10 K/min through the main crystallization peak, kept at 473 K for 90 minutes and cooled subsequently at 10 K/min. The two exothermic peaks were clearly observed, albeit in two stages. Considering the overall process as one broad, two-stage event and estimating a total area clearly yields too large ΔH_{total} values, much larger than the average heat of fusion from Table 3. The two peaks must correspond to two separate events. The main peak is the crystallization that occurs with a supercooling of about 30 K. Its heat most likely corresponds to the heat of fusion of Table 3 (always slightly lower on cooling than on heating). The heat of crystallization goes through a maximum when plotted vs cooling rate. The smaller peak is absent for the fastest and the slowest cooling rates. In the latter case a broad, downward-curved process is apparent over the whole temperature range, but its area, if considered as a broad exotherm, is too large to justify it being a thermal effect. The area for the peak is almost constant for the four continuous experiments, but more than doubles in the case of the two-stage experiment. The peak temperature decreases only on cooling at 80 K/min, while the separation of the two peak temperatures is almost constant, about 70 K.

An additional comparison of mc and sc samples can be made in terms of their heat capacity. The most direct comparison is to run an sc sample through its melting transition, cool at a slow rate and reheat the resulting sample that is now mc. This method eliminates all inadvertent differences between the two samples. Such a comparison is shown in Fig. 9. The initial run clearly shows the Brill transition, as has been described in detail above. On reheating, the heat capacity starts increasing immediately above T_g and is much higher than that of the sc sample in the vicinity of the Brill transition. The glass transition is

also much broadened and shifted to a higher temperature.

The comparison for the heat capacities of runs *s*5 and *m*8 is shown in Fig. 10. The samples had been annealed for a long time at 493 K and were then cooled slowly. The Brill transition is seen for run *s*5 and an endotherm appears also in run *m*8 that was absent in Fig. 9. Sample *m*8 has a higher C_p than *s*5 and the area of the broad endothermic process of *m*8 is comparable, if not larger, in latent heat, than the area under the distinct peak ascribed to the Brill transition of *s*5.

Discussion

The Brill transition

The Brill transition can be defined as a gradual change to a higher-symmetry form as evidenced by the changes in the x-ray diffraction pattern with increasing temperature. We think that it occurs qualitatively in both sc and mc samples in the same way. The associated endothermic effects as seen by DSC are, however, different.

The distinct endothermic peak of the sc samples before melting was fully characterized thermally by the DSC experiments described. The average peak temperature 466.4 K and heat 2.44 kJ/mol that we determined are different than the values quoted by Starkweather [15], namely 473 K and 4.26 kJ/mol, respectively. Even if the slight difference in crystallinity, as inferred from the different measured heats of fusion, is taken into account to adjust for 100 % crystallinity, the latent heats still do not match. Given that the samples of Starkweather were crystallized from methanol under autogenous pressure, we can conclude that the transition is strongly dependent on the quality of the crystals grown and on the crystallization conditions. Our results show only small deviations from the average values. Once the sample is crystallized from solution, the peak is not changed much by thermal treatment and is perfectly reversible, as experiment *s*6 shows, without changes in heat or temperature of transition. Annealing for a long time above the transition, as performed in experiment *s*5, showed that while melting was affected, there was no change for the Brill peak. Apparently, reorganization in the crystals grown from solution does not affect the transition. Experiment *s*7 also showed that cooling from above the transition as fast as 500 K/min had no effect, as can be seen on reheating. The transition is too fast to be affected by such quenching rates.

The WAXD data (Fig. 1) indicate that the Brill transition occurs in mc samples in spite of the lack of a distinct peak in the DSC trace. We think that the thermal effect associated here with the transition is a broad endotherm extending over the whole region between T_g and T_m. This broad endotherm for nylon 6.6 is a feature that was noted in our earlier experiments and was not associated with the Brill transition. In the case of experiment *m*1, described in detail in [9], the endotherm was the explanation of why the melting range was so wide; it was especially evident for nylon 6.6 compared to the other nylons. In fact, the cooling rate has a bigger effect on nylon 6.6 than on the other nylons, the C_p being higher for the lower cooling rates. The same was noted in experiment *m*10. The endotherm is also seen in all other DSC experiments on mc samples described in this work. Figures 9 and 10 show quite clearly that both sc and mc samples have an endothermic effect that is different in nature.

The uniformity of the crystals is perhaps the main reason why a clearer maximum is seen in the heat capacity curve at the Brill transition for the sc samples. SAXS data obtained on both samples [20] show that, compared to mc samples, they have a much sharper peak; the peak is centered at an angle corresponding to a *d*-spacing closer to the optimum lamellar thickness [6]. We think that the transition is associated with a change in packing that occurs in a more uniform way than in the mc samples. This change in packing can be followed from the expansivity results obtained in [21]. The crystalline specific volume increases by 12 % from room temperature to 470 K. The increase is almost exponential. Above 470 K the specific volume remains surprisingly constant and then increases abruptly as melting occurs. A review of expansivity data on crystals collected in [22] indicates that, for all semicrystalline polymers studied, the increase in specific volume from the lowest temperature measured to about 50 K below the melting temperature of each polymer ranges typically from 1 % to 7 %. The only exception is polytetrafluoroethylene (PTFE), where the increase is 16 % over 250 K. It is well established, however, that PTFE is a condis crystal above room temperature [23]. The volume increase in that case is due to torsional oscillations and hindered rotations about the chain axis in the hexagonal condis phase. When compared to all other polymers analyzed, the expan-

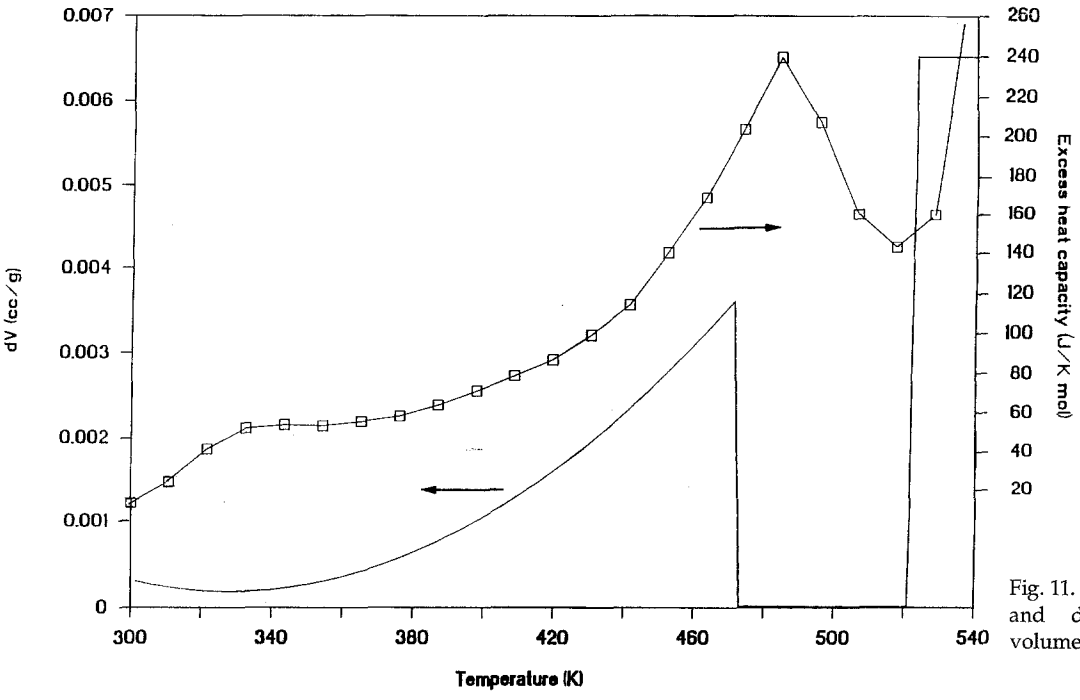

Fig. 11. Excess heat capacity and differential specific volume for sc nylon 6.6

sivity (volume increase per degree) for nylon 6.6 is only smaller than that for polyethylene. The increase for polyethylene is gradual and is also associated with conformational disorder [23]. A volume increase of about 5 % was found in the case of polydiethylsiloxane for the transition from a rigid crystal to a condis crystal using molecular mechanics calculations [24]. The added volume was needed to accommodate the large-amplitude ethyl group librations and gauche bond sequences. Even on fusion, changes in volume for typical polymers are only 10–15 % [25], the same order of magnitude observed for nylon 6.6.

The expansivity data from [21] were further analyzed by digitizing the published specific volume plot and fitting to a third-order polynomial (293–473 K) and two straight lines (474–523 K and 523–528 K). The differential volume, dV, was then plotted versus temperature along with the excess heat capacity, defined as the experimental C_p*) minus the C_p computed for the nylon under the condition of exclusively vibrational motion.

The comparison is shown in Fig. 11; a close correspondence is obvious. The increase in C_p with a maximum at 480 K, followed by a renewed approach to the vibrational heat capacity before melting follows the expansivity (dV) behavior. The decrease in expansivity comes about because, once the hexagonal symmetry is reached, large-amplitude librations do not cause further defects in the packing. The pseudohexagonal crystal form, ultimately reached, has such a structure with an almost cylindrical symmetry allowing freer motion about the chain axis.

Both the expansivity and the heat capacity data are corroborated by quasielastic neutron-scattering data collected on sc samples of nylon 6.6 [26]. The observed broadening of the elastic peak and appearance of a Lorentzian component are interpreted as evidence of large-amplitude motions of the protons in the methylene groups of nylon 6.6. At 500 K, 40 K below melting, the protons are already moving at a frequency of 1.1×10^{11} Hz. It could be shown that the motions involved are local in nature with essential retention of long-range order. This microscopic picture is in agreement with the motions inferred by the other two macroscopic methods. It is also in agreement with the NMR results discussed in the Introduction.

The important effect in the solid-state properties of nylon 6.6 is the gradual introduction of conformational disorder in the crystals; this transformation

*) The data are for the solution-crystallized sample, already shown in Fig. 9.

is followed by the packing change, which seems overall not to be a first-order transition. As proven by x-ray analysis, both effects occur in both sc and mc samples. The fact that a "Brill transition" is not seen in other nylons is only incidental and is related to the higher melting point of nylon 6.6. More specifically, the ability of nylon 6.6 to shift into a more symmetrical crystal form reduces the driving force for melting and, as a result, increases its melting point. In the case of other nylons the details of the crystal structure are such that a packing reorganization is not favored. The crystals go from the condis state directly into the melt. In fact, the gradual convergence of the two main x-ray diffraction peaks with increasing temperature is quite a common phenomenon in nylons. Melting, however, intervenes before the two peaks actually merge.

Effects of thermal history

In order to be able to characterize the Brill transition and the associated thermal effects, we need to study the effect of annealing and crystallization on the ultimate thermal behavior. The experiments performed show that the Brill transition in sc samples is not much affected by thermal treatment, unlike the mc samples that are very much affected. They also show that the observed increase in heat capacity is not due to premelting and reorganization.

Some effects were seen in the case of experiments *s*1 and *s*2. The difference between the two experiments was the heating rate to the annealing temperature T_a, being slow for *s*1 and fast for *s*2. We wanted to see the relative importance of heating to T_a and time spent at T_a. The systematic differences observed show the former to be more important. Both peak temperature and transition heat were higher for *s*1 compared to *s*2 for both the melting and the Brill transitions. Clearly a fast heating rate to T_a hinders reorganization on heating, an effect not compensated by 30 min at T_a. The effect is much more pronounced for the Brill transition. Although the transition is not affected by annealing above the transition temperature, it is affected by the rate at which T_a was reached. The reorganization on heating, and thus the ultimate quality of the crystals, defines the endothermic effect seen at the Brill transition. A minimum is seen for ΔH_{Brill} at T_a = 480 K in both *s*1 and *s*2. This annealing temperature is very close to the Brill peak temperature on the high-temperature side. Staying at a temperature where the process is occurring with most intensity apparently disrupts it to an extent evidenced in subsequent heating. A comparable effect is not seen at a temperature symmetrically below the Brill peak temperature.

An interesting temperature dependence is seen by comparing the two data sets on powder mc samples, shown in Fig. 1. The transition occurs between 400 K and 440 K on heating, as estimated by the merging of the two main peaks. On cooling from 493 K the transition starts around 380 K and continues down to room temperature. The process is similarly gradual on heating. The increase of the intensity of the 010, 110 reflection after having heated to 493 K (see Fig. 2a) can be interpreted as an increase in ordering of the hydrogen-bonded planar sheets. This is contrasted with premelting that occurs on heating at 523 K (see Figure 2b): the resulting pattern has a 010, 110 reflection that is now of lower intensity than in the unannealed sample. Presumably, the poor crystals were molten and could not reform properly on cooling. This experiment proves that premelting has a very different effect than the onset of conformational mobility.

The WAXD experiments of Fig. 3, performed on the quenched samples, need a different interpretation. The transition on heating occurs at a lower temperature when compared to Fig. 1, namely between 380 K and 400 K. On cooling after reaching 460 K the surprising effect is that the transition occurs at a higher temperature, between 430 K and 410 K. Without change in crystal size, one would expect any transition to occur on cooling with a certain supercooling. This effect was also seen for the transition in question in the original work by Brill [11]. What we observe here must be an effect of annealing, in agreement with the DSC results from experiment *m*3, which will be discussed below. The poor, quenched crystals reorganize on heating and go into the pseudohexagonal phase at a lower temperature. As they reorganize and improve on heating, the transition is moved to higher temperatures. Although not performed, a subsequent heating should show that the transition will occur at a higher temperature, comparable to that shown in Fig. 1.

This WAXD behavior of the quenched samples is similar to the DSC behavior observed in experiment *m*3 (see Fig. 6). The initial heating curve to 520 K shows a broad endotherm, centered around 400 K. On cooling (see Fig. 7) the corresponding exotherm is seen at a higher temperature, about 420 K. Reheating has the corresponding endotherm at 450 K. Sub-

sequent cycling does not change the exotherms and endotherms any further. The broad endotherm on heating is seemingly related to the Brill transition, in agreement with the WAXD results. In fact, the run *m*4–3, which refers to a quenched sample, shows the broad endotherm in the same temperature range where the WAXD changes occur. It has to be noted that sample *m*4–3 was not as effectively quenched as sample *m*1-*Q* so that no exotherm is seen above T_g.

Of course, reorganization of poor crystals into better ones may also account for the endothermic effects between T_g and T_m. Experiment *m*8, however, shows that, in fact, these two processes exist in parallel and are distinguishable. Annealing for a long time clearly improved the crystals, giving the highest ΔH_m value of Table 3 and producing the most distinct double peak of all experiments. The double peak is due to the fact that the annealing temperature was not high enough to give the highest-melting crystals. The improvement of the crystals when largely completed, did not remove the broad endotherm in the temperature range from 350 K to 500 K. The area under the endotherm reaches 2.2 kJ/mol, a value comparable to the area of the Brill transition. The endotherm should thus not be a manifestation of reorganization on heating. The distinction of increased C_p from premelting was also found for all other nylons studied [9]. It was noted also that the increase was beginning too early to be explained by premelting. In addition, the systematic dependence of T_1 (the temperature where C_p^{exp} crosses the C_p of the melt) on thermal history was opposite of what would have been expected by premelting.

An additional proof of the different behavior of annealing peaks and increase in heat capacity due to conformational disorder can be found in experiment *m*2, shown in Fig. 5. The small peak, whose temperature increases linearly with crystallization temperature, is clearly an annealing peak [27] caused by recrystallization at T_c of a small population of poor crystals that melt on subsequent reheating. The experimental heat capacities indicate an additional systematic effect, namely the broad endotherm appearing before the annealing peak and being most pronounced for the best crystals and highest crystallinity, i.e., the highest T_c. The broad endotherm cannot thus be assigned to reorganization, the latter process being related to the annealing peak.

On cooling from the melt the sample can either crystallize directly into the triclinic form or first crystallize into the pseudohexagonal form and then transform to the triclinic one. In the cooling curve seen in Fig. 8 we note two exothermic processes. The area under the small low-temperature peak is about 50 % larger than the area expected for the Brill transition. This may be due to the very wide temperature range of the exotherm on cooling. If the area under the heat capacity is considered over the same temperature range as on heating, the areas on heating and on cooling become comparable. The two processes can therefore be assigned to a crystallization through the pseudohexagonal into the triclinic form. This assignment is further corroborated by the two-stage run. The large increase in the area under the secondary peak is caused by the complete crystallization to the pseudohexagonal form achieved during the stay at 473 K. The transition to the triclinic form then involves many more, and better, pseudohexagonal crystals.

The lack of a low-temperature exothermic process for the fastest- and the slowest-cooled samples is due to two different effects. In the case of the fast cooling rate it is caused by a combination of extremely high supercooling and lack of instrument sensitivity at such fast rates. Temperature control is not retained during most of the run and certainly not towards the end of it. In the case of the slow rate the explanation is a physical one: the sample goes directly to the triclinic form. As cooling is performed close to equilibrium, the best possible crystals are formed with no intermediate step.

Conclusions

1. Aliphatic nylons exhibit, above their glass transition, a gradual increase in heat capacity linked to conformational disorder in the crystals.

2. Wide-angle x-ray diffraction experiments on melt-crystallized nylon 6.6 samples of different crystallinity show that the Brill transition occurs in all cases. They also revealed that annealing during heating shifts the transition to higher temperature.

3. The Brill transition in nylon 6.6 is associated with a broad endotherm between T_g and T_m in melt-crystallized samples, and develops a distinct endothermic peak in solution-crystallized samples. This is supported by comparison of the heat capacities of the two samples.

4. The Brill transition is not a true, first-order transition. It is only an incidental thermal effect associated with packing changes in the crystal. The

onset of conformational disorder is a gradual effect, separable from premelting, and is evidenced by the large increase in volume. In the high-temperature pseudohexagonal form there is no volume increase because of its higher symmetry.

Acknowledgements

This research was sponsored by the Division of Materials Research of the National Science Foundation, Polymers Program, Grant # DMR-8818412 and by the Division of Materials Sciences, Office of Basic Energy Sciences, U.S. Department of Energy, under Contract DE-AC05-84OR21400 with Martin Marietta Energy Systems, Inc. Thanks are given to Professor Stephen Z. D. Cheng (University of Akron) for the x-ray data in Fig. 3, and to Dr. Brian Annis (Oak Ridge National Laboratory) for the SAXS data mentioned in the discussion.

References

1. Clark ES, Wilson FC (1973) In: Kohan MI (ed) Nylon Plastics. Academic Press, New York, p 271
2. Starkweather Jr HW (1973) In: Kohan MI (ed) Nylon Plastics. Academic Press, New York, p 307
3. Bunn CW, Garner EV (1947) Proc Roy Soc London 189A:39
4. Bell JP, Slade PE, Dumbleton JH (1968) J Polym Sci Part A-2 6:1773
5. Todoki M, Kawaguchi T (1975) J Polym Sci Polym Phys Ed 15:1067
6. Dreyfuss P, Keller A (1970) J Macromol Sci-Phys B4:811
7. Slichter WP (1958) J Polym Sci 35:77
8. Xenopoulos A, Wunderlich B (1990) Polymer 31:1260
9. Xenopoulos A, Wunderlich B (1990) J Polym Sci Polym Phys Ed to appear
10. Wunderlich B, Grebowicz J (1984) Adv Polym Sci 60/61:1
11. Brill R (1942) J Prakt Chem 161:49
12. Schmidt GF, Stuart HA (1958) Z Naturforschung 13a:222
13. Olf HG, Peterlin A (1971) J Polym Sci A-2 9:1449
14. Wendoloski JJ, Gardner KH, Hirschinger J, Miura H, English AD (1990) Science 247:431
15. Starkweather Jr HW, Jones GA (1981) J Polym Sci Polym Phys Ed 19:467
16. Starkweather Jr HW (1989) Macromolecules 22:2000
17. Magill JH, Girolamo M, Keller A (1981) Polymer 22:43
18. Loufakis K, Wunderlich B (1987) J Polym Sci Polym Phys Ed 25:2345
19. Ginnings DC, Furukawa GT (1953) J Am Chem Soc 75:522
20. Xenopoulos A (1990) PhD Thesis Rensselaer Polytechnic Institute Troy New York (data taken with Dr. Brian Annis)
21. Starkweather Jr HW, Zoller P, Jones GA (1984) J Polym Sci Polym Phys Ed 22:1615
22. Pan R, Varma-Nair M, Wunderlich B (1989) J Therm Anal 35:955
23. Wunderlich B, Möller M, Grebowicz J, Baur H (1988) Adv Polym Sci 87:1
24. Miller KJ, Grebowicz J, Wesson JP, Wunderlich B (1990) Macromolecules 23:849
25. Wunderlich B (1980) Macromolecular Physics Volume 3 Academic Press New York
26. Xenopoulos A, Wunderlich B, Trouw F, Narten AH, in preparation
27. Illers KH (1969) Makromol Chem 127:1

Received May 14, 1990
accepted June 20, 1990

Authors' address:

Prof. B. Wunderlich
Dr. A. Xenopoulos
Dept. of Chemistry
University of Tennessee
Knoxville, Tennessee 37996-1600, USA